Ivo DOLEŽEL[1], Václav KOTLAN[1], Bohuš ULRYCH[1]

University of West Bohemia in Pilsen, Czech Republic (1)

Modeling of Induction Shrink Fit of Action Wheel in Gas Turbine

Abstract. *Induction shrink fit in a gas turbine is modeled. The fit is realized by pressing of a heated steel wheel carrying the blades on shaft and its purpose is to transfer a relatively high torque in specific operation conditions. The paper deals with the numerical solution of the process that represents a nonlinear and nonstationary coupled problem characterized by interaction of magnetic field, temperature field and field of thermoelastic displacements. The methodology is illustrated by a typical example whose results are discussed.*

Streszczenie. *Zaproponowano modelowanie indukcyjnego dopasowania koła w turbinie gazowej. Dopasowanie to polega na naprężaniu rozgrzanego koła w celu ułatwienia transferu dużego momentu. Przedstawiono model numeryczny procesu uwzględniający pola magnetyczne i temperaturpowe oraz odkształcenie termoelastyczne. (**Modelowanie indukcyjnego dopasowania wymiarów koła w turbinie gazowej**)*

Keywords: induction shrink fit, coupled problem, numerical analysis, magnetic field, temperature field, thermoelastic displacements.
Słowa kluczowe: dopasowanie indukcyjne, analiza numeryczna, zjawiska termoplastyczne.

Introduction

One of the most mechanically and thermally exposed parts of gas turbines are blade-carrying wheels rotating at high velocities in very hot environment. These wheels are fixed to a shaft by means of shrink fits. Every shrink fit has to transfer a relatively high torque, which is secured by an appropriate interference whose selection must also take into account the centrifugal force acting on the wheel and environmental temperature.

The process of hot pressing leading to the shrink fit starts with induction heating of the wheel. This brings about an enlargement of the diameter of its internal hole, the wheel is put on the shaft and the whole system is cooled. The particular steps of the process are depicted in Fig. 1.

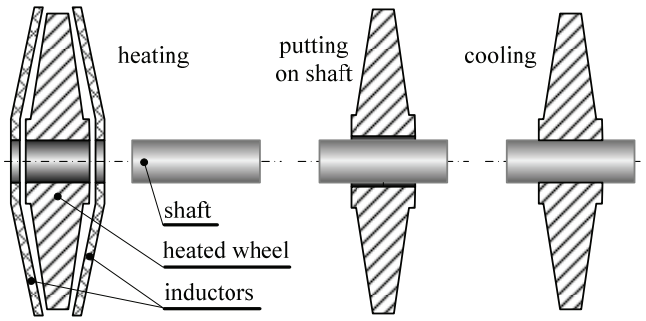

Fig. 1. Particular steps of the process

As the above process requires a lot of energy, its consumption is desirable to be minimized. And this necessitates selection of a suitable arrangement of the field coils (in other words selection of either transverse or longitudinal magnetic field) and also selection of the amplitude and frequency of the field current.

From the physical viewpoint, the task represents a triply coupled nonlinear and nonstationary problem with mutual interaction of electromagnetic field, temperature field and field of thermoealstic displacements. The papers dealing with its solution are still rather rare. In [1] the authors solved a similar problem in a weakly coupled formulation; other tasks of this type were tackled, for example, in [2].

The aim of this work is to carry out a complete study of preparation of the above shrink fit, determine the time evolution of displacements of selected points of the wheel and find the efficiency of the process.

Formulation of the technical problem

Consider an arrangement of the wheel and shaft depicted in Fig. 2. The wheel is heated by two coils (indicated in the right part of the Figure) in two variants providing the transversë (up) and longitudinal (down) magnetic fields. The coils can be planar, conical, but even more sophisticated shapes are used in the industrial practice. They are mostly formed by a massive hollow copper conductor cooled by water.

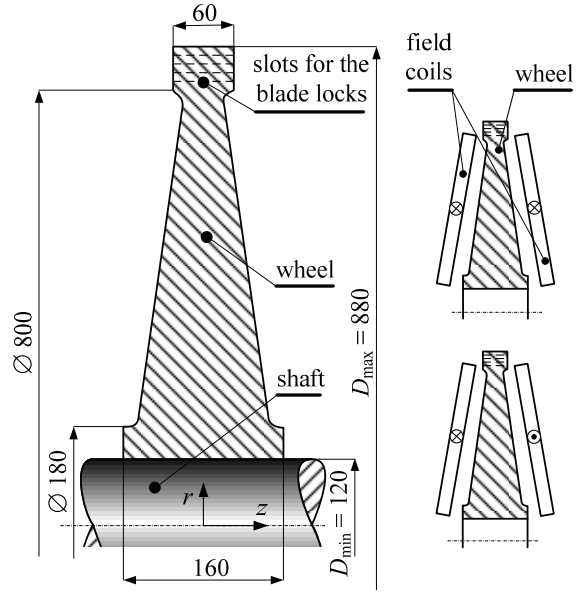

Fig. 2. Arrangement of the system wheel – shaft (left) and two possible arrangements of the inductors in the process of heating (right): up–producing transverse magnetic field, down–producing longitudinal magnetic field

The aim of this paper is to build a sufficiently realistic mathematical model of the process of heating, to solve it for the given geometry and material parameters and to evaluate the possibilities of reducing the amount of energy necessary for reaching the required displacements. Our efforts can be summarized in the following items:

- Proposal of the mathematical model and its numerical realization.
- Estimation of parameters of the field current that produces a sufficient dilatation of the bore in an acceptable time period.
- Mapping of the complete process of heating for both transverse and longitudinal magnetic fields and its overall evaluation.

Mathematical model of the process

Magnetic field in the system produced by the field coils is described (due to the presence of nonlinearities) by the

well-known parabolic equation for magnetic vector potential $\boldsymbol{A}$ in the form [3]

$$\operatorname{curl}\left(\frac{1}{\mu}\operatorname{curl}\boldsymbol{A}\right)+\gamma\frac{\partial\boldsymbol{A}}{\partial\boldsymbol{t}}=\boldsymbol{J}_{\mathrm{ext}}, \tag{1}$$

where μ denotes the magnetic permeability, γ is the electric conductivity and $\boldsymbol{J}_{\mathrm{ext}}$ stands for the vector of the external harmonic current density in the field coil.

But solution to equation (1) is practically unfeasible. The reason consists in the deep disproportion between the frequency f (tens or hundreds Hz) of the field current and time of heating (usually several minutes). That is why the model was somewhat simplified using the assumption that the magnetic field is harmonic. In such a case it can be described by the Helmholtz equation for the phasor $\underline{\boldsymbol{A}}$ of the magnetic vector potential $\boldsymbol{A}$

$$\operatorname{curlcurl}\underline{\boldsymbol{A}}+\mathrm{j}\cdot\omega\gamma\mu\underline{\boldsymbol{A}}=\mu\underline{\boldsymbol{J}}_{\mathrm{ext}}, \tag{2}$$

where ω is the angular frequency. On the other hand, magnetic permeability in any cell of the discretization mesh covering ferromagnetic domains is assigned to the local value of magnetic flux density.

The conditions along the axis of the device and artificial boundary placed at a sufficient distance from the system are of the Dirichlet type ($\underline{\boldsymbol{A}}=\underline{\boldsymbol{0}}$).

The temperature field in the system is described by the heat transfer equation [4]

$$\operatorname{div}\left(\lambda\cdot\operatorname{grad}T\right)=\rho c_{\mathrm{p}}\cdot\frac{\partial T}{\partial t}-w, \tag{3}$$

where λ is the thermal conductivity, ρ denotes the mass density and c_{p} stands for the specific heat at a constant pressure (all of these parameters are temperature-dependent functions). Finally, symbol w denotes the time average volumetric sources of heat that generally consist of the volume Joule losses w_{J} due to eddy currents and magnetization losses w_{m}, so that

$$w=w_{\mathrm{J}}+w_{\mathrm{m}}, \tag{4}$$

where

$$w_{\mathrm{J}}=\frac{\left|\underline{\boldsymbol{J}}_{\mathrm{eddy}}\right|^2}{\gamma},\quad \underline{\boldsymbol{J}}_{\mathrm{eddy}}=\mathrm{j}\cdot\omega\gamma\underline{\boldsymbol{A}}, \tag{5}$$

while the losses w_{m} (if they are considered) are determined from the known measured loss dependence $w_{\mathrm{m}}=w_{\mathrm{m}}\left(\left|\underline{\boldsymbol{B}}\right|\right)$ for the used material (as the magnetic vector potential $\boldsymbol{A}$ is harmonic, magnetic flux density $\boldsymbol{B}$ in every element is in this model also harmonic).

The boundary conditions should take into account convection and radiation, but their particular application depends on the case solved.

The solution of the thermoelastic problem may be carried out using several approaches. After a thorough analysis we decided for the Lamé equation, whose application seems to be the most convenient (from the viewpoint of the numerical processing). This equation reads [5]

$$\begin{aligned}&\left(\varphi+\psi\right)\cdot\operatorname{grad}\left(\operatorname{div}\boldsymbol{u}\right)+\psi\cdot\Delta\boldsymbol{u}-\\&-\left(3\varphi+2\psi\right)\cdot\alpha_{\mathrm{T}}\cdot\operatorname{grad}T+\boldsymbol{f}=\boldsymbol{0},\end{aligned} \tag{6}$$

where $\varphi>0,\ \psi>0$ are coefficients associated with material parameters by the relations

$$\varphi=\frac{\nu\cdot E}{\left(1+\nu\right)\left(1-2\nu\right)},\ \psi=\frac{E}{2\cdot\left(1+\nu\right)}. \tag{7}$$

Here, E denotes the modulus of elasticity and ν is the Poisson number of the transverse contraction. The modulus of elasticity generally depends on the actual temperature. Finally, $\boldsymbol{u}=\left(u_r,u_z\right)$ represents the displacement vector, α_{T} the coefficient of the thermal dilatability of material (which is also a temperature-dependent function) and $\boldsymbol{f}$ denotes the vector of the internal volumetric (electromagnetic, gravitational) forces. The application of the boundary conditions depends on the arrangement solved, but in general, no axial displacement of the longitudinal axis of the wheel is considered due to its perfect symmetry.

Computer model

The numerical solution of the problem is realized by a fully adaptive finite element method [6], whose algorithms are implemented into codes Hermes2D [7] and Agros2D [8] that have been developed in our group for several years.

The codes written in C++ are intended for monolithic numerical solution of systems of generally nonlinear and nonstationary second-order partial differential equations whose principal purpose is hard-coupled modeling of complex physical problems. While Hermes is a library containing the most advanced procedures and algorithms for the numerical processing of the task solved, Agros represents a powerful preprocessor and postprocessor. Comprehensive information about them can be found on www pages. Both codes are freely distributable under the GNU General Public License. Their most important (and in some cases quite unique) features follow:

- Solution of the system of PDEs (rewritten into the weak formulation) is carried out in the monolithic form (which means that the resultant numerical scheme is characterized by just one stiffness matrix).
- Fully automatic *hp*-adaptivity. In every iteration step the solution is compared with the reference solution (realized on an approximately twice finer mesh), and the distribution of error is then used for selection of candidates for adaptivity [9–10].
- Each physical field is solved on quite a different mesh that best corresponds to its particulars. This is of great importance, for instance, for respecting skin effect in the electromagnetic field, boundary layers in the field of flow etc. In nonstationary processes every mesh can change in time, in accordance with the real evolution of the corresponding physical quantities.
- Easy processing of the hanging nodes [11] appearing on the boundaries of subdomains whose elements have to be refined. Usually the hanging nodes bring about a considerable increase of the number of the degrees of freedom (DOFs). The code contains higher-order algorithms for respecting these nodes without any need of an additional refinement of the external parts neighboring with the refined subdomain.
- Curved elements able to replace curvilinear parts of any boundary by a system of circular or elliptic arcs. These elements allow reaching highly accurate results near the curvilinear boundaries with very low numbers of DOFs.

Illustrative example

A wheel made of carbon steel CSN 12 040, whose dimensions are specified in Fig. 2, was heated in order to increase its internal bore by $\Delta D_{\min}=0.9$ mm.

For illustration, Fig. 3 shows the magnetization characteristic of the above material and Figs. 4–6 depict the nonlinear temperature dependencies of its electric conductivity γ, thermal conductivity λ, and heat capacity ρc_p [12]. On the other hand, the elastic parameters of this carbon steel are considered constant: the Young modulus is $E = 2.1\times10^{11}$ N/m^2, the Poisson number $\nu = 0.3$ and the coefficient of thermal dilatability $\alpha_\mathrm{T} = 1.25\times10^{-5}$ K^{-1}.

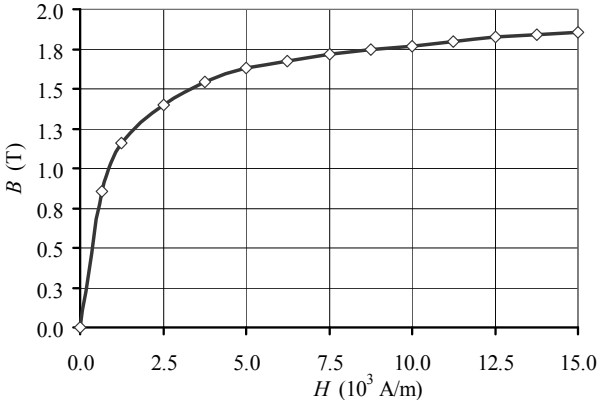

Fig. 3. Magnetization curve of carbon steel CSN 12 040

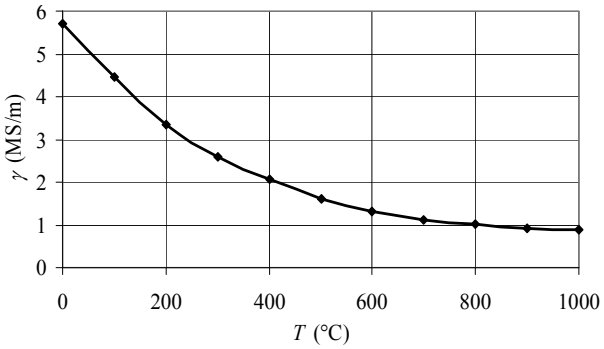

Fig. 4. Dependence of $\gamma = \gamma(T)$ for carbon steel CSN 12 040

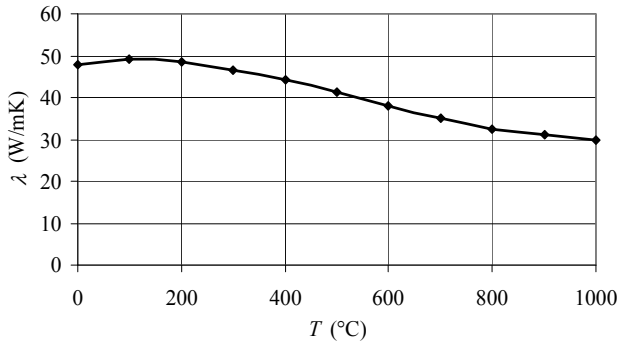

Fig. 5. Dependence of $\lambda = \lambda(T)$ for carbon steel CSN 12 040

Both inductors are wound by a massive hollow copper conductor in an arrangement depicted in Fig. 7. Each of them has 15 turns and the conductors are cooled by water flowing inside. The inductors are packed in glass wool in order to reduce the thermal losses by convection and radiation from the heated wheel. This means that the wheel is thermally well insulated in the course of its heating, except for a small part at the place of the blades.

The distributions of the volumetric Joule losses in the heated wheel for both transverse and longitudinal magnetic fields look very similarly. At low temperatures they are concentrated (even for low frequencies) in its surface layers due to both skin effect and high permeability of material. When the temperature of the wheel (due to its good thermal conductivity and a relatively long time of heating it is very uniform) exceeds about 400 °C, the permeability starts decreasing and the layers with Joule losses become thicker.

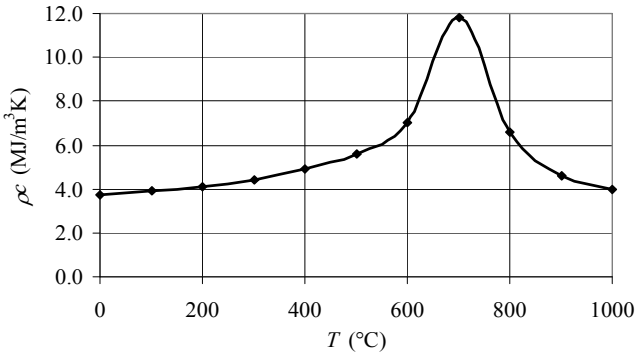

Fig. 5. Dependence of $\rho c_\mathrm{p} = \rho c_\mathrm{p}(T)$ for carbon steel CSN 12 040

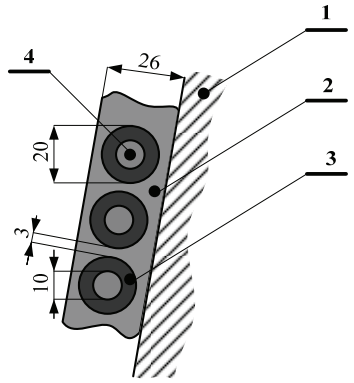

Fig. 7. Arrangement of the inductor (dimensions in mm): **1**–heated wheel, **2**–glass wool, **3**–turns of the inductor, **4**–cooling water

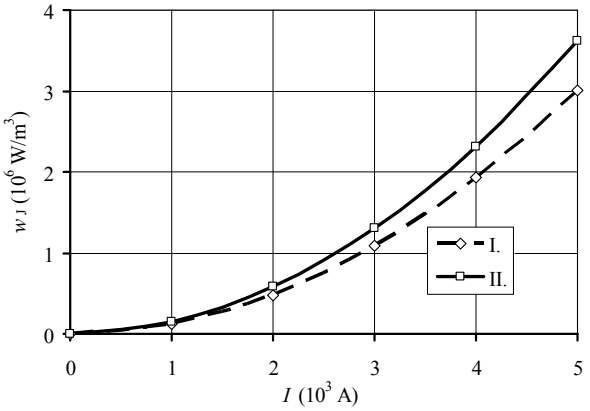

Fig. 8. Dependence of the average volumetric Joule losses in the wheel at the room temperature on the field current (I – longitudinal field, II – transverse field, $f = 50$ Hz)

But despite the above qualitative similarity, there are quantitative differences between both ways of heating. Figure 8 shows, for example, the dependence of the average volumetric Joule losses w_J in the heated wheel on the field current I ($f = 50$ Hz) at the room temperature ($T = 20$ °C). The full line shows the corresponding dependence for the transverse field, the dashed one for the longitudinal field. And such curves behave similarly even for higher temperatures. It is clear, that from the viewpoint of the velocity of heating and total efficiency of the process the transverse field is more favorable.

Figure 9 shows the time evolution of the temperature of the wheel for field current of amplitude $I = 5 \times 10^3$ A, and frequency $f = 50$ Hz in case of the longitudinal field. Analogously, Fig. 10 shows the same distributions for the transverse field.

Even here we can see that heating in the transverse magnetic field is somewhat faster (by about 10%). Finally, Fig. 11 depicts the time evolution of the minimum radial displacement u_r of the internal bore of the wheel.

We can see that the required displacement $\Delta D_{\min} / 2 = 0.45$ mm is in case of the transverse field reached in about 15 minutes of heating, which is the time well agreeing with experiments and real experience reached at various manufacturers of shrink fits.

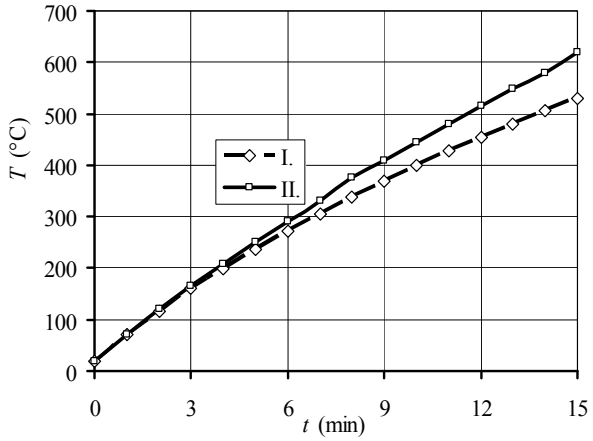

Fig. 9. Time evolution of the temperature of the heated disk in the longitudinal magnetic field for $I = 5 \times 10^3$ A and $f = 50$ Hz: I – the average temperature of the disk, II – the average temperature of the internal surface of the bore of the disk

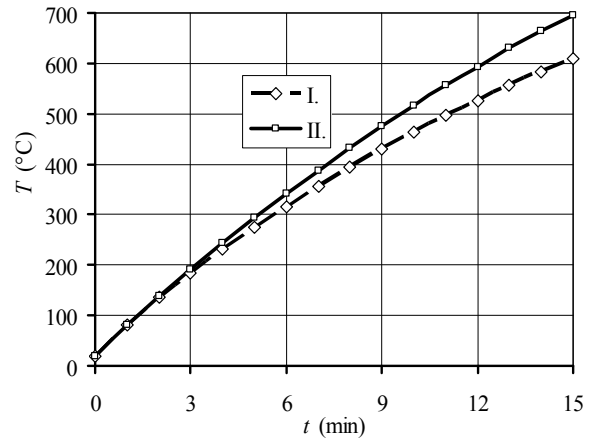

Fig. 10. Time evolution of the temperature of the heated wheel in the transverse magnetic field for $I = 5 \times 10^3$ A and $f = 50$ Hz: I – the average temperature of the disk, II – the average temperature of the internal surface of the bore of the disk

Conclusion

For the investigated wheel, heating in the transverse magnetic field exhibits higher parameters and better efficiency than in the longitudinal one. Further acceleration of the process may be reached after thermal insulating the upper part of the action wheel in a similar way how the sides of the wheel were insulated for the presented analysis.

Next work in the field will be focused on further improvement of numerical algorithms and acceleration of the computations. After finding the temperature dependencies of the mechanical parameters (E, ν, α_T) of the steel, they will also be included in the analysis.

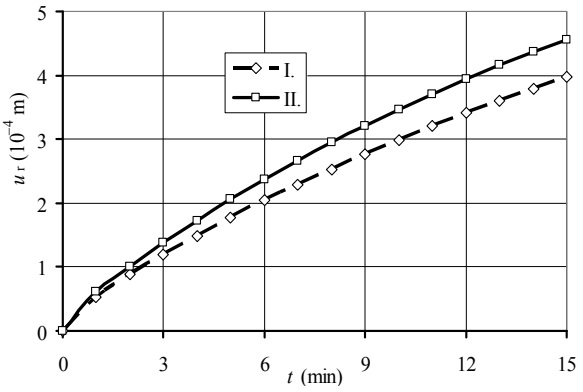

Fig. 11. Time evolution of the minimum radial displacement of the internal bore of the wheel for $I = 5 \times 10^3$ A and $f = 50$ Hz (I – longitudinal field, II – transverse field)

Acknowledgment

This work was supported by the European Regional Development Fund and Ministry of Education, Youth and Sports of the Czech Republic (project No. CZ.1.05/2.1.00/03.0094: Regional Innovation Centre for Electrical Engineering – RICE) and by Grant projects GACR 102/09/1305 and GACR P102/11/0498.

REFERENCES

[1] Skopek, M., Ulrych, B., Dolezel, I. (2003) "Optimized regime of induction heating of a disk before its pressing on shaft", *IEEE Trans. Magn.*, Vol. 37, No. 5, pp. 3380–3383.

[2] Mun, C. S., Kwang, K. J., Kyo, J. H., Gyun, L. C. (2001) "Stress and thermal analysis coupled with field analysis of multi-layer buried magnet synchronous machine with a wide speed range", *IEEE Trans. Magn.*, Vol. 39, No. 3, pp. 1265–1268.

[3] Stratton, J. A. (2007), *Electromagnetic Theory*, John Wiley & Sons, Inc., Hoboken, NJ.

[4] Holman, J. P. (2002), *Heat Transfer*, McGrawHill, New York, USA.

[5] Boley, B., Wiener, J. (1960), *Theory of Thermal Stresses*, Wiley, New York, USA.

[6] Solin, P., Segeth, K., Dolezel, I. (2003), *Higher-Order Finite Element Methods*, Chapman & Hall/CRC, Boca Raton, USA.

[7] http://agros2d.org.

[8] http://hpfem.org/hermes/.

[9] Solin, P., Dubcova, L., Kruis, J. (2010) "Adaptive *hp*-FEM with dynamical meshes for transient heat and moisture transfer problems", *J. Comput. Appl. Math.,* Vol. 233, No. 12, pp. 3103–3112.

[10] Dubcova, L., Solin, P., Cerveny, J., Kus, P. (2010) "Space and time adaptive two-mesh *hp*-FEM for transient microwave heating problems", *Electromagnetics*, Vol. 30, No. 1, pp. 23–40.

[11] Solin, P., Cerveny, J., Dolezel, I. (2008), "Arbitrary-level hanging nodes and automatic adaptivity in the hp-FEM", *Math. Comput. Simul.,* Vol. 77, No. 1, pp. 117–132.

[12] Company Standard SKODA 00 6004 (in Czech).

***Authors**: Ivo Doležel, Václav Kotlan and Bohuš Ulrych, Department of Theory of Electrical Engineering, Faculty of Electrical Engineering, University of West Bohemia, Univerzitni 26, 306 14 Plzen, Czech Republic, E-mail: {idolezel, vkotlan, ulrych}@kte.zcu.cz.*